



Article scientifique

Article

2021

Published version

Open Access

This is the published version of the publication, made available in accordance with the publisher's policy.

Computational Study of Benzosultam Formation through Gold(I)-Catalyzed Ammoniumation/Nucleophilic Substitution Reaction

Pertschi, Romain; de Aguirre, Adiran; Pale, Patrick; Blanc, Aurélien; Poblador Bahamonde, Amalia Isabel

How to cite

PERTSCHI, Romain et al. Computational Study of Benzosultam Formation through Gold(I)-Catalyzed Ammoniumation/Nucleophilic Substitution Reaction. In: Helvetica Chimica Acta, 2021, vol. 104, n° e2100133. doi: 10.1002/hlca.202100133

This publication URL: <https://archive-ouverte.unige.ch/unige:155561>

Publication DOI: [10.1002/hlca.202100133](https://doi.org/10.1002/hlca.202100133)



Computational Study of Benzosultam Formation through Gold(I)-Catalyzed Ammoniumation/Nucleophilic Substitution Reaction

Romain Pertschi,^a Adiran de Aguirre,^a Patrick Pale,^b Aurélien Blanc,^{*b} and Amalia I. Poblador Bahamonde^{*a}

^a Department of Organic Chemistry, University of Geneva, CH-1211 Geneva, Switzerland, e-mail: amalia.pobladorbahamonde@unige.ch

^b Institut de Chimie, UMR 7177 – CNRS, University of Strasbourg, FR-67070 Strasbourg, France, e-mail: ablanc@unistra.fr

Dedicated to Prof. E. Peter Kündig on the occasion of his 75th birthday

© 2021 The Authors. Helvetica Chimica Acta published by Wiley-VHCA AG. This is an open access article under the terms of the Creative Commons Attribution Non-Commercial License, which permits use, distribution and reproduction in any medium, provided the original work is properly cited and is not used for commercial purposes.

The Au(I)-catalyzed reactions of (2-alkynyl)phenylsulfonyl azetidines bearing terminal and non-terminal alkynes in the presence of methanol as protic nucleophile to form benzosultams derivatives were studied by density functional theory (DFT) calculations. Our study highlights that gold(I) catalyzed nucleophilic addition of the nitrogen on the alkyne is favored over the direct ring opening of the azetidine by methanol, confirming the ammonium-based mechanism. In addition, the reverse regioselectivity observed experimentally where non-terminal alkynes favors the formation of 6-endo-dig-benzosultams while terminal alkynes favor 5-exo-dig products is also explored through two different scenarios. The first one embraces the classical activation of the alkyne by a single Au(I) species while the second one tackles the formation of a σ,π -digold acetylide complex. Calculations identify both pathways as competitive although only mono Au(I) complexes can lead to final products, in good agreement with experimental observation. Further details on the importance of the presence of an excess of the protic nucleophile on the protodemetalation step and the final aminal formation is also discussed.

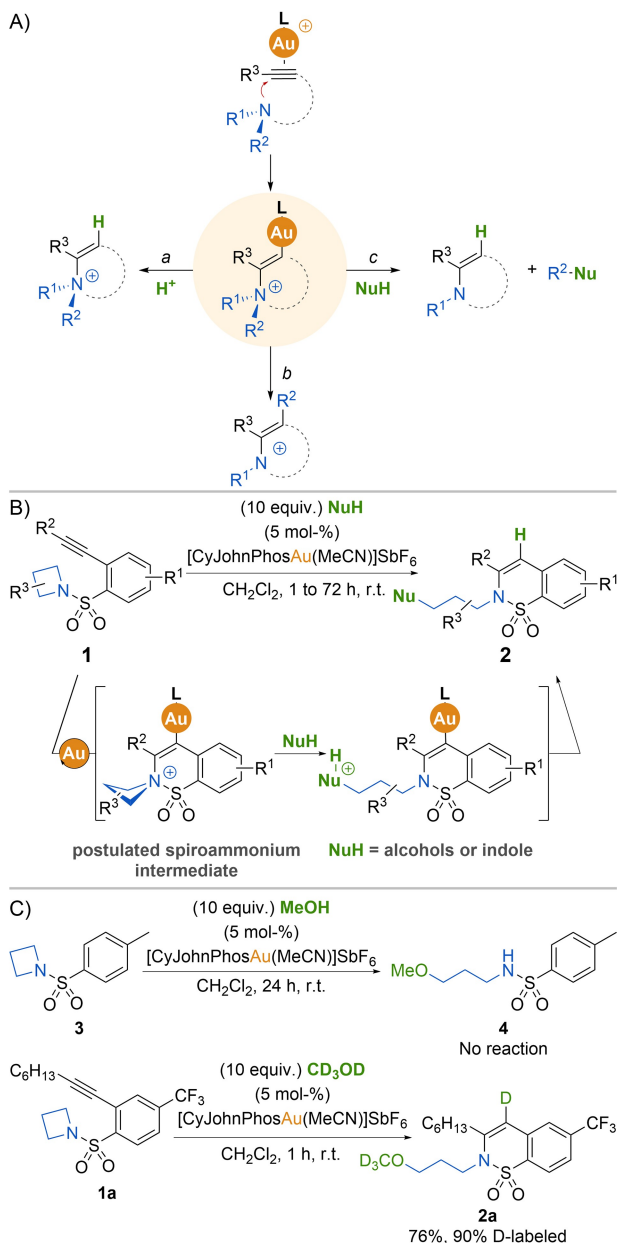
Keywords: benzosultam formation, cascade reaction, density functional calculations, gold(I) catalysis, reaction mechanisms.

Introduction

Since the beginning of the century, gold has undoubtedly become the star metal to promote nucleophilic additions to unsaturated carbon–carbon bonds, especially alkynes.^[1–3] The large relativistic effect impacting this element confers to gold(I) cation a strong π -Lewis acidity.^[4–7] Thus, gold(I) provided a powerful tool towards the elaboration of complex carbo and heterocycles and especially towards the formation of nitrogen containing heterocycles through intramolecular

nucleophilic addition of primary or secondary amine on a gold-activated insaturation.^[8–10] The protic nature of the amine allows the protodemetalation to readily occur through the release of a proton from the so-formed vinyl-ammonium-gold(I) species, ensuring the regeneration of the catalyst.^[11–14] If instead of primary or secondary amine a tertiary amine is used, no proton can be generated by the nucleophile itself and the resulting vinyl-ammonium-gold(I) intermediate is blocked at this stage.^[15] Three different strategies can be considered to ensure the regeneration of the catalyst: 1) the addition of a strong acid to force the demetallation step^[16] (Scheme 1, A, path a), or 2) a sigmatropic rearrangement (Scheme 1, A, path b) or 3) the ammonium can be intercepted by a protic

Supporting information for this article is available on the WWW under <https://doi.org/10.1002/hlca.202100133>



Scheme 1. A) Strategies used for the regeneration of Au(I) species from vinyl ammonium-gold(I) intermediate; Postulated mechanism (B) and mechanistic experiments (C) for the synthesis of benzosultam from (2-alkynyl)phenylsulfonyl azetidine. CyJohnPhos = 2-(Dicyclohexylphosphino)biphenyl.

nucleophile (Scheme 1,A, path c). These two last appealing approaches open the way to new cascade reactions leading to highly sophisticated aza-cyclic structures and was already harnessed in various transformations.^[17–24] Recently, we described a series of cascade reaction based on the so-called gold(I)-catalyzed ammoniation strategy combined with the peculiar reactivity of azetidines. Thus, starting with

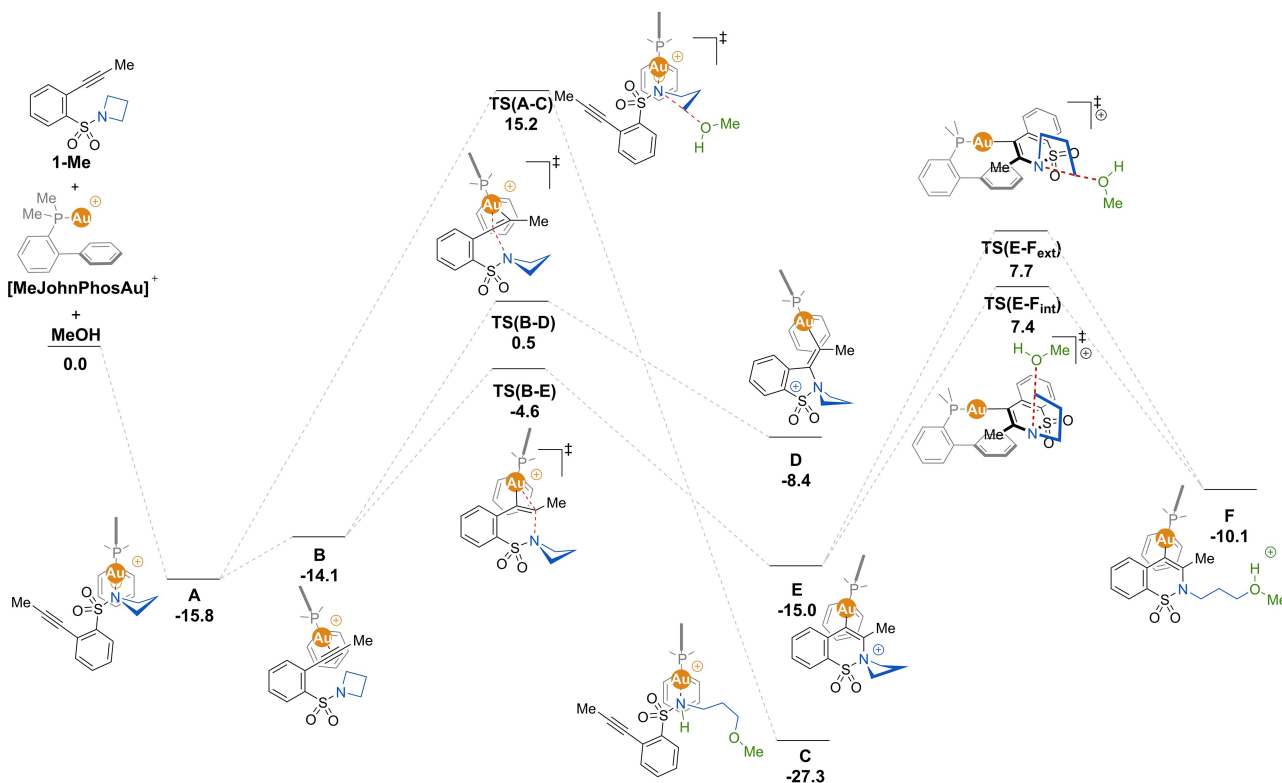
similar azetidine derivatives, a large variety of sophisticated azacyclic structures could be reached such as hydroazepines, pyrroles, pyrrolizines, pyrrolin-4-ones and carbapenem derivatives.^[25–30] It is worth mentioning that clear evidence of the involvement of a vinyl-ammonium-gold(I) intermediate was settled in such cyclization.

To extend this concept of gold(I)-catalyzed ammoniation, we recently described the gold(I)-catalyzed formation of benzosultams **2** from an original starting material, the (2-alkynyl)phenylsulfonyl azetidines **1** in the presence of a protic nucleophile (Scheme 1,B).^[31] The postulated mechanism for this reaction proceeds through a nucleophilic addition of the nitrogen on the alkyne leading to a spirocyclic vinyl-ammonium-gold(I) intermediate that can then react with a protic nucleophile by ring opening of the azetidine moiety. To assess the proposed mechanism a series of experiments, including isotopic labelling, were performed (Scheme 1,C). The azetidine analog **3** lacking the alkyne group did not evolve toward the ring opened product **4** in the presence of gold(I) catalyst and an excess of methanol. This experiment revealed the necessity of the alkyne moiety to ensure the ring opening of the azetidine. The reaction performed with (D₄)methanol as nucleophile starting from alkynyl azetidine derivative **1a** gave the benzosultam **2a** deuterated at the expected position according to the proposed mechanism.

However, no clear evidence could be provided to attest of the formation of spirocyclic vinyl-ammonium-gold(I) intermediate which could never be observed by NMR or isolated using stoichiometric amount of gold(I). Furthermore, regioselective issues appeared while switching from non-terminal to terminal alkynes. To decipher the mechanism of the benzosultam formation, the system was computationally studied, and the results are described herein.

Results and Discussion

All calculations were carried out using Gaussian 09^[32] software at the DFT level of theory. Optimization of the structures were performed using the hybrid functional B3LYP including Grimme dispersion model D3.^[33–36] The effective-core potential valence basis set LANL2DZ^[37] was used to describe Au and the other atoms were described by the 6–31G** basis set.^[38–44] Thermal corrections to the Gibbs free energy were obtained at the same level of theory. Single-point energy calculations were carried out using the same



Scheme 2. Free energy reaction profile (kcal/mol) for the ammoniation/nucleophilic substitution step using **1-Me** as substrate computed at B3LYP-D3(DCM)/LANL2TZ(f)/6-311++G**//LANL2DZ/6-31G** level of theory. Computed geometries for the transition states of the ring opening of the azetidine are shown in boxes.

functional with the triple- ζ valence LANL2TZ(f)^[45] basis set on Au and the 6-311++G**^[46] basis set on other elements. To account for the solvation energy the SMD model was used (dichloromethane, $\epsilon = 8.93$) on both, optimizations and single point calculations. All reported data are Gibbs free energies given in kcal·mol⁻¹ at 298 K and 1 atm. All optimized structures were characterized by frequency analysis either as energy minima without imaginary frequencies or with only one imaginary frequencies for transition states. To ensure the reliability of the transition states found, the latter were linked to their product through intrinsic reaction coordinate (IRC) analysis.^[47,48]

To set up a reliable computational model for the reaction, **1-Me** (Scheme 2) was used as model substrate¹ and (2-biphenyl)-dimethylphosphine (MeJohn-

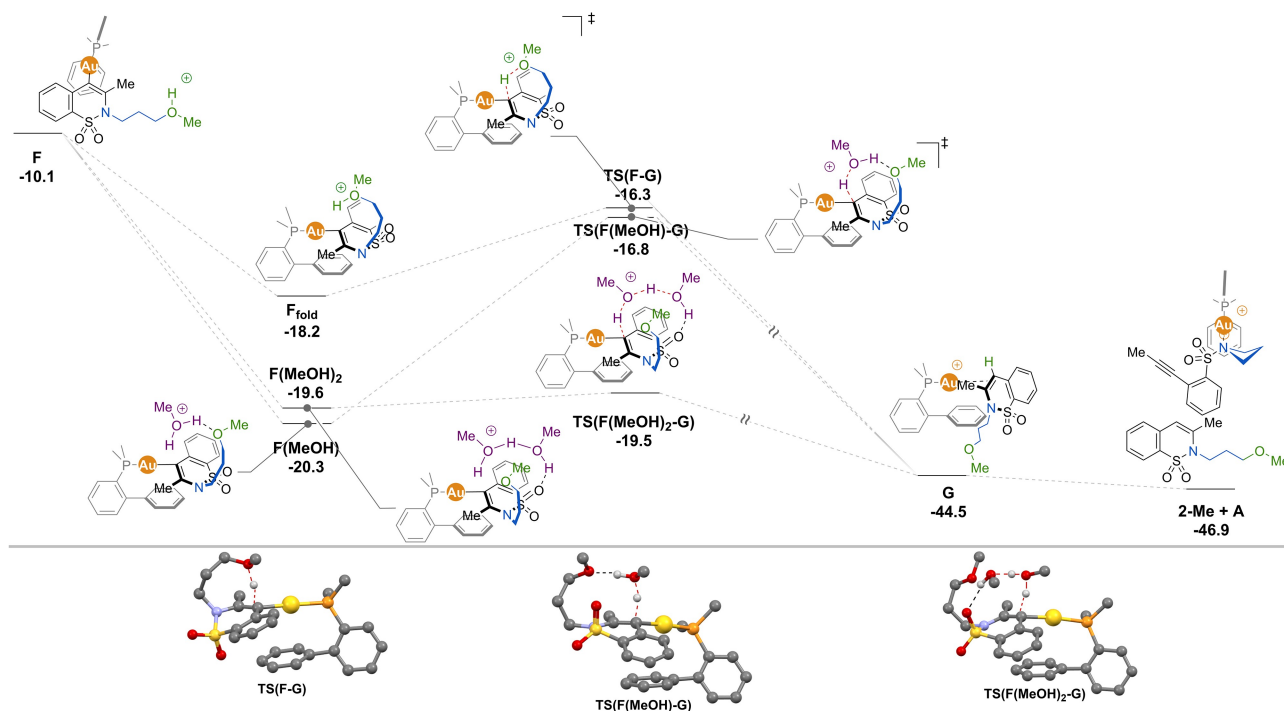
Phos) as a model ligand for the cationic gold complex.^[49,50] Scheme 2 shows the reaction profile for the ammoniation reaction followed by nucleophilic substitution of the (2-alkynyl)phenylsulfonyl azetidine **1-Me** in the presence of the gold catalyst. The reaction starts with the coordination of the gold complex $[\text{MeJohnPhosAu}]^+$ to the nitrogen lone pair of the azetidine **1-Me** leading to the very stable intermediate **A** lying at -15.8 kcal·mol⁻¹. The formation of **A** is favored over the coordination of the alkyne (**B**) by 1.7 kcal·mol⁻¹. At this stage, two different scenarios can be considered: 1) the direct ring opening of the azetidine by methanol (**A** to **C**) and 2) the expected nucleophilic addition of the nitrogen to the activated triple bond (**B** to **D** or **B** to **E**). The former was discarded as the formation of **C** involves a high barrier of 31.0 kcal·mol⁻¹ via **TS(A-C)**, confirming our initial assumption where the mechanism is based on a gold (I) catalyzed ammoniation process. Therefore, the following C–N bond formation from **B** was computed through both, the 6-endo-dig (**B** to **E**) and the 5-exo-dig (**B** to **D**) ammoniation process. The 6-endo-dig cyclization is clearly favored over the 5-exo-dig by an

¹The alkyl chain attached to the alkyne is replaced by a methyl group in order to avoid conformation issues and to reduce computational time. The aryl substituent was replaced by a proton due to its low impact on the reaction process.

energy difference of $\Delta\Delta G^\ddagger = 5.1 \text{ kcal}\cdot\text{mol}^{-1}$ in the transition state and a $\Delta\Delta G = 6.6 \text{ kcal}\cdot\text{mol}^{-1}$ over the product. This result is in full agreement with the experimental observation where no five membered ring **D** was observed on non-terminal alkynes. The next step of the reaction consists in the ring opening of the azetidine moiety of the spirocyclic vinyl-ammonium-gold(I) species **E** by a methanol molecule. This step proceeds through a S_N2 mechanism leading to the ring opening of the azetidine moiety (**E** to **F**). Due to the desymmetrization of the system induced by the MeJohnPhos ligand, two different transition states, **TS(E-F_{ext})** and **TS(E-F_{int})**, were found for the ring opening of the azetidine since the two electrophilic carbons of the azetidine become non-equivalent. The approach of the nucleophile from the slightly less sterically hindered position of the azetidine via **TS(E-F_{int})** is favored by only $0.3 \text{ kcal}\cdot\text{mol}^{-1}$. This step is the rate limiting step with an activation barrier of $22.4 \text{ kcal}\cdot\text{mol}^{-1}$, affordable at the experimental conditions (Nucleophile (10 equiv.), [CyJohnPhosAu (MeCN)]SbF₆ (5 mol-%), CH₂Cl₂, room temperature, 1–72 h) and depicts well the experimental behavior of the system where the steric and the electronic properties of the nucleophile drastically influence the reac-

tion rate. The protonated gold sultam **F** is found at $-10.1 \text{ kcal}\cdot\text{mol}^{-1}$.

The protodemetalation step from intermediate **F** is shown in *Scheme 3*. First, a direct intramolecular demetalation was computed. This step occurs through a refolding of the methoxypropyl chain allowing the approach of the cationic moiety towards the carbon stabilizing the complex by $7.7 \text{ kcal}\cdot\text{mol}^{-1}$ (**F_{fold}**). In this disposition, the proton transfer occurs through **TS(F-G)** and requires an activation barrier of $1.9 \text{ kcal}\cdot\text{mol}^{-1}$. This step yields complex **G** at $-44.5 \text{ kcal}\cdot\text{mol}^{-1}$. Owing to the presence of an excess of methanol in the mixture, the addition of one/two explicit methanol molecules was considered to assist this demetalation process.^[51] The addition of the first explicit methanol molecule led to the formation of a cationic MeOH₂⁺ which favors the proton transfer through **TS(F(MeOH)-G)** transition state. Our efforts to locate the concerted version of this transition state were unsuccessful. Finally, the inclusion of a second methanol molecule led to the formation of intermediate **F(MeOH)₂**. As previously observed, the proton of the side chain is already transferred to the methanol dimer however, in this case, the second methanol molecule favors hydrogen bonding with the sulfoxide moiety. Then, the final proton transfer transition state,



Scheme 3. Free energy reaction profile (kcal/mol) for the protodemetalation step using **1-Me** as substrate computed at the B3LYP-D3(DCM)/LANL2TZ(f)/6-311 + +G**//LANL2DZ/6-31G** level of theory.

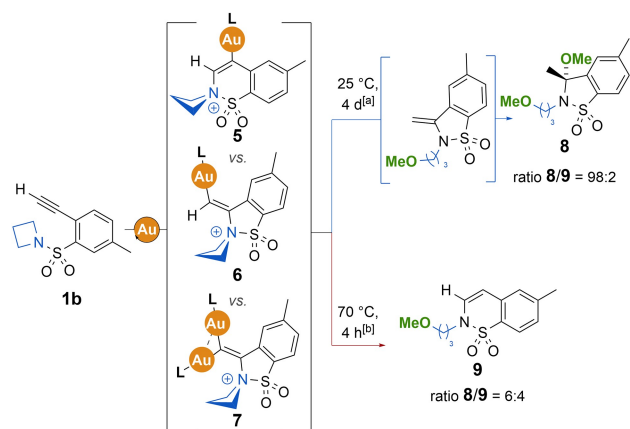
TS(F(MeOH)₂-G) led to the carbon–gold bond cleavage through a barrier-free process. The inclusion of explicit molecules of methanol in the calculations are key to stabilize the system and to promote the proton transfer even if the non-assisted process is also competitive. The assistance of the methanol for this step can be considered as both intermolecular as the proton is first transferred to the solvent and then transferred back to the molecule, and intramolecular through a refolding of the ether arm. This step could also be promoted by a second intermediate **F**. This hypothesis was not considered due to the low activation barriers previously discussed and the huge steric hindrance of the system. The final release of the sultam product **2-Me** from the gold complex and the coordination of a new molecule of **1-Me** is favored by 2.4 kcal·mol⁻¹, closing the catalytic cycle. The overall process from reactants to product is highly exergonic by 46.9 kcal·mol⁻¹.

If the use of (2-alkynyl)phenylsulfonyl azetidines bearing a substituted alkyne experimentally led only to the formation of six-membered ring benzosultams **2**, the use of a terminal alkyne (**1b**) led almost exclusively to the five-membered ring sultam aminal **8** (Scheme 4). It is worth to mention that now the reaction is very slow at room temperature and needs the use of the nucleophile as a co-solvent.² Interest-

ingly, raising the temperature up to 70 °C reduces the reaction time although a loss of selectivity towards **9** is observed. Indeed, the ratio between **8** and **9** switches from 98:2 at 25 °C to 6:4 at 70 °C. ¹H-NMR showed that aminal **8** could unambiguously arise from a 5-*exo*-dig pathway. The favored 5-*exo*-dig pathway at lower temperature is consistent with the known gold-catalyzed cyclization of terminal alkynes^[52] and suggest the possible involvement of a σ,π -digold acetylide complex in the mechanism.^[53–57] Thus, two distinct pathways can be considered to explain the observed temperature dependent regioselectivity: 1) the monogold pathway involving the formation of a five- (**6**) or six- (**5**) membered ring spirocyclic vinyl-ammonium-gold(I) species or, 2) the digold pathway involving the formation of a spirocyclic vinyl-ammonium-digold(I) (**7**) species.^[58,59]

Up to here, the small MeJohnPhos model ligand was used. Nevertheless, since the formation of σ,π -digold acetylide species was considered, the steric hindrance generated by both ligands on both gold complexes may play a role on the ammoniation/nucleophilic substitution step of **1-H**. Therefore, and in order to evaluate its impact on the selectivity as well as on possible conformational restrictions, the full CyJohnPhos³ ligand was used.^[60]

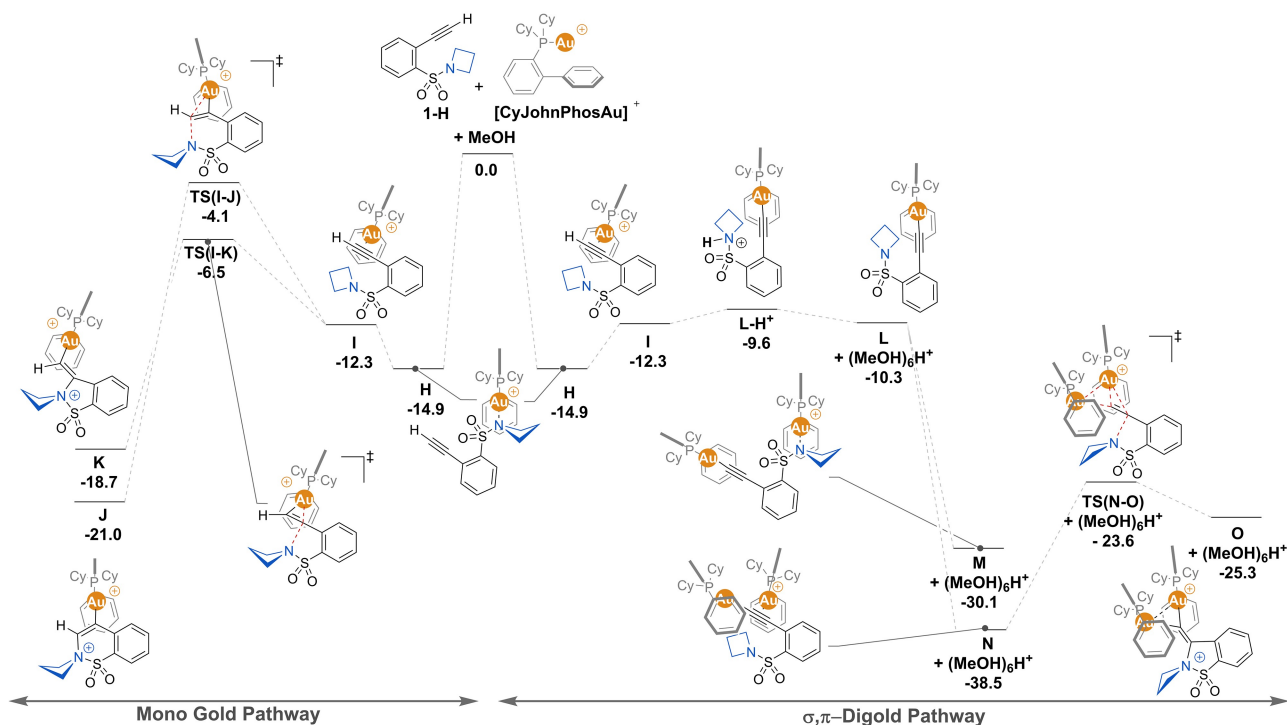
Scheme 5 shows both scenarios starting by the coordination of **1-H** to the gold complex [CyJohnPhosAu]⁺ through the nitrogen lone pair of the azetidine moiety leading to the very stable intermediate **H** lying at –14.9 kcal·mol⁻¹. As previously discussed, this coordination mode is slightly favored over the alkyne (**I**) by 2.6 kcal·mol⁻¹ (see Scheme 2 for comparison with the [MeJohnPhosAu]⁺ system). This monogold complex then evolves to the ammoniation step through the 6-*endo*-dig (Scheme 5, **I** to **J**) or the 5-*exo*-dig cyclization (Scheme 5, **I** to **K**). In contrast to previous calculations with non-terminal alkyne, the 5-*exo*-dig is slightly favored over the 6-*endo*-dig with an energy difference of $\Delta\Delta G^\ddagger = 2.4$ kcal·mol⁻¹ in the transition state. This result agrees with experimental observation where the five membered ring (**8**) is favored over the six membered ring (**9**).



Scheme 4. Temperature dependence on the regioselectivity of the reaction while using a terminal alkyne on the (2-alkynyl) phenylsulfonyl azetidine (**1b**).^[a] Reaction performed with: [CyJohnPhosAu(MeCN)]SbF₆ (5 mol-%), MeOH/CH₂Cl₂ (1:1), 20 °C, 4d.^[b] Reaction performed with: [CyJohnPhosAu(MeCN)]SbF₆ (10 mol-%), (10 equiv.) MeOH, CH₂Cl₂, 70 °C, 4 h.

²Using the standard conditions (10 equiv. of MeOH) leads to the formation of the desired aminal **8**. However, the reaction is very slow.

³The initial structure of the [CyJohnPhosAu] (Scheme 5) used to set up the calculation was taken from the crystal structure of the [CyJohnPhosAu(MeCN)]SbF₆.



Scheme 5. Free energy reaction profile (kcal/mol) for the ammoniation step involving mono- and di-gold species using **1-H** as substrate computed at the B3LYP-D3(DCM)/LANL2TZ(f)/6-311 + G**//LANL2DZ/6-31G** level of theory. Computed geometry for the transition state of the di-gold ammoniation step is shown in the box.

On the digold scenario, the intermediate **I** evolves towards the formation of the gold acetylide **L** which requires addition of a cluster of solvent molecules to allow its deprotonation⁴. After the deprotonation, a second gold complex can coordinate the system. Two coordination modes were considered; on the nitrogen of the azetidine or on the alkyne (**M** vs. **N**, respec-

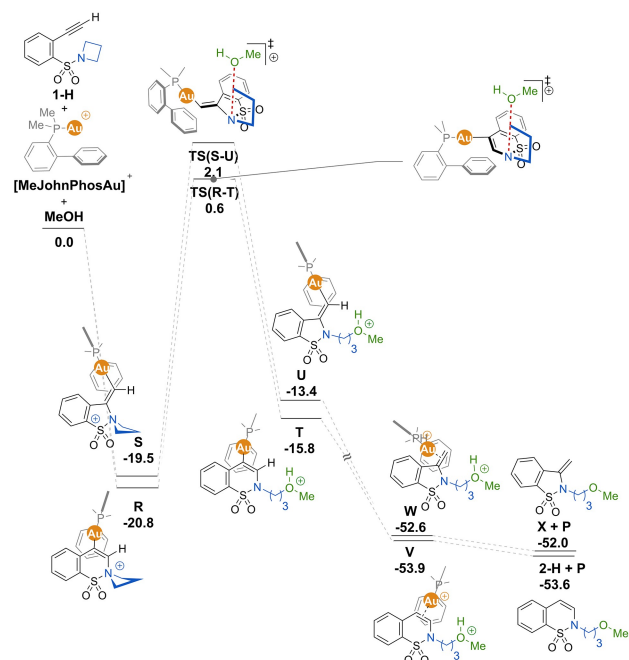
tively). Coordination of the gold complex into the triple bond is favored by $8.4 \text{ kcal}\cdot\text{mol}^{-1}$ and stabilizes the system by $28.2 \text{ kcal}\cdot\text{mol}^{-1}$.

The calculated ammoniation step requires a barrier of $14.9 \text{ kcal}\cdot\text{mol}^{-1}$ and yields the five membered ring complex **O**, at $-25.3 \text{ kcal}\cdot\text{mol}^{-1}$. Any attempt to locate the transition state for the six membered ring product was unsuccessful. Interestingly, this digold pathway confirms the feasibility of the ammoniation process, in agreement with the experimentally observed selectivity of the reaction. The full reaction profile was additionally computed using the smaller MeJohnPhos model (see Schemes 6 and 7 and Schemes S13, S14). Both systems behave in the same manner, therefore, and in order to decrease the complexity of the system, the smaller MeJohnPhos ligand was further used.

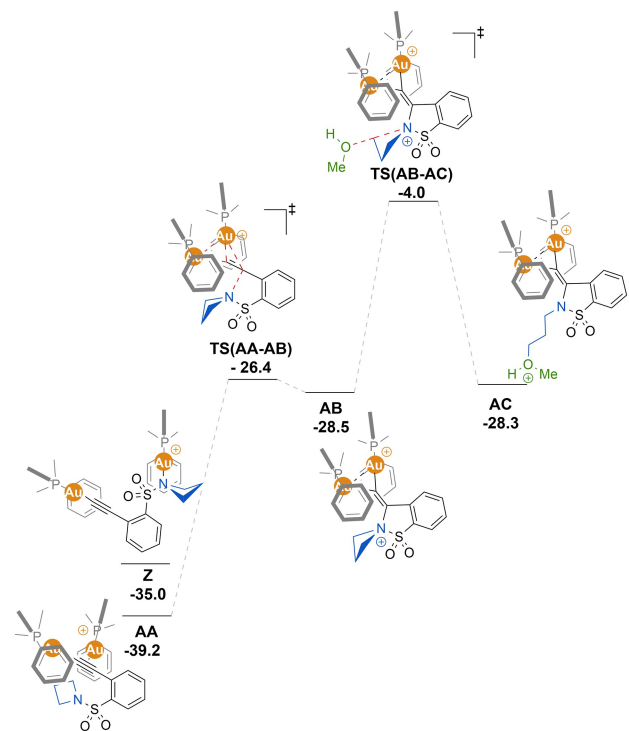
A short version with the key steps of the reaction profile of the monogold pathway with terminal alkyne **1-H** as substrate is depicted in Scheme 6.⁵ The formation of the vinyl-ammonium-gold(I) species **R**

⁴The intermediate **I** evolves towards the formation of the gold acetylide **L-H⁺** through deprotonation of the alkyne and protonation of the azetidine due to its basicity. The following deprotonation of the azetidine moiety may be assisted by methanol as it is experimentally used as a co-solvent. Therefore, calculations of one, three and six molecules of methanol to catalyze the process were considered. The use of the monomer $(\text{MeOH})\text{H}^+$ and the trimer $(\text{MeOH})_3\text{H}^+$ led to a destabilization of the complex by 25.0 and $3.7 \text{ kcal}\cdot\text{mol}^{-1}$ respectively, whereas the consideration of the cyclic hexamer stabilized $(\text{MeOH})_6\text{H}^+$ the system by only $0.7 \text{ kcal}\cdot\text{mol}^{-1}$. This small energy difference highlights both, the acid/base equilibrium, and the importance of a methanol cluster to redeem the nucleophilic nitrogen required for the further ammoniation step (see full reaction pathway on Scheme S2 in the Supporting Information).

⁵See full reaction pathway on Scheme S13 in the Supporting Information.



Scheme 6. Free energy reaction profile (kcal/mol) for the [MeJohnPhos] mono-gold complex with **1-H** as substrate computed at the B3LYP-D3(DCM)/LANL2TZ(f)/6-311++G**//LANL2DZ/6-31G** level of theory.



Scheme 7. Free energy reaction profile (kcal/mol) for the [MeJohnPhos] di-gold complex with **1-H** as substrate and $(\text{MeOH})_6\text{H}^+$ cluster computed at the B3LYP-D3(DCM)/LANL2TZ(f)/6-311++G**//LANL2DZ/6-31G** level of theory. **1-H** and [MeJohnPhosAu]⁺ are used as zero.

and **S** follow the same behavior than those computed with the full system.⁶ The ammoniation process yields the 6-membered (**R**) and the 5-membered (**S**) ring ammonium intermediate, but the first is slightly thermodynamically favored over the second ($\Delta\Delta G = 1.3 \text{ kcal}\cdot\text{mol}^{-1}$).⁷ The following ring opening of the azetidine by methanol was computed and similar barriers were located. The protonated gold(I)-sultam intermediates, **T** and **U**, rapidly undergo protodemetalation leading to the formation of the very stable complexes **V** and **W** lying at 53.9 and $52.6 \text{ kcal}\cdot\text{mol}^{-1}$ below the initial reactants, respectively. Finally, the coordination of a new molecule of **1-H** to gold promotes the release of both sultams **X** and **2-H**, in a highly exergonic process ($-53.9 \text{ kcal}\cdot\text{mol}^{-1}$ for **2-H** and $-52.0 \text{ kcal}\cdot\text{mol}^{-1}$ for **X**).

Previous calculations of digold species with the CyJohnPhos ligand feature specific conformational restrictions. Taken those into account, similar geometries were used for the MeJohnPhos ligand to mimic accurately the full system, even if they do not represent the most stable conformation on the latter model. The full reaction profile for the process involving **1-H** is depicted in Scheme 7.⁸ From intermediate **AA**, the nucleophilic addition of the nitrogen into the alkyne followed by the opening of the azetidine moiety to reach the formation of 5-membered ring sultam **AC** requires an overall activation barrier of $35.2 \text{ kcal}\cdot\text{mol}^{-1}$. This high activation barrier highlights the unviability of this step at the experimental conditions. Hence, the digold pathway can be

⁶These results are in accordance with the initial assumption that the steric hindrance of the cyclohexyl substituents plays a minor role on the monogold pathway and can be replaced by methyl groups in the calculation without any remarkable impact.

⁷In terminal alkynes, the formed spirocyclic vinyl-ammonium-gold(I) species **R** and **S** are clearly favored over the reactant **P** by an energy difference of 4.7 and $3.4 \text{ kcal}\cdot\text{mol}^{-1}$ for **R** and **S**, respectively suggesting that these intermediates could be potentially isolable.

⁸The addition of the second gold complex bearing the MeJohnPhos ligand in the calculation only led to a small energy difference compared to the full system. Thus, the ammoniation step occurs with a comparable barrier, $12.8 \text{ kcal}\cdot\text{mol}^{-1}$ instead of $14.9 \text{ kcal}\cdot\text{mol}^{-1}$, for the MeJohnPhos and CyJohnPhos systems, respectively. These results emphasize the limited impact of the steric hindrance induced by the Cy groups of the phosphine and that the main steric interaction comes from its biphenyl substituent.

discarded as a possible scenario for the formation of the 5-membered ring sultam **X**.

The detail analysis of the digold scenario show that the formation of the σ,π -digold acetylide **AA** is competitive to the ammoniumiation step catalyzed by monogold species (see *Schemes S13* and *S14* in the *Supporting Information*). This observation not only confirms the slow kinetic at room temperature but is also consistent with the lack of reactivity reported in the literature regarding these digold species.^[61,62]

Interestingly, the final methylene sultam **X** was only observed by ¹H-NMR in the crude reaction mixture. Its isolation led to the formation of the aminal upon evaporation or column chromatography. To understand the overall process, calculations of the mechanism by gold catalyzed species were run but found to be unsuccessful⁹. Therefore, a metal free pathway was considered, and the most favored process found is shown in *Scheme 8*. The methylene sultam intermediate proceeds through a concerted six-membered ring transition state involving two molecules of methanol, with an activation barrier of 26.4 kcal·mol⁻¹, leading to the slightly more stable aminal product **AE**.¹⁰ This activation barrier could be potentially lowered by the addition of more explicit methanol in the calculations, stabilizing the transition state through hydrogen bond interactions. It is thus clear that the aminal formation occurs through a classical enamine protonation process, in agreement again with the experimental observation.

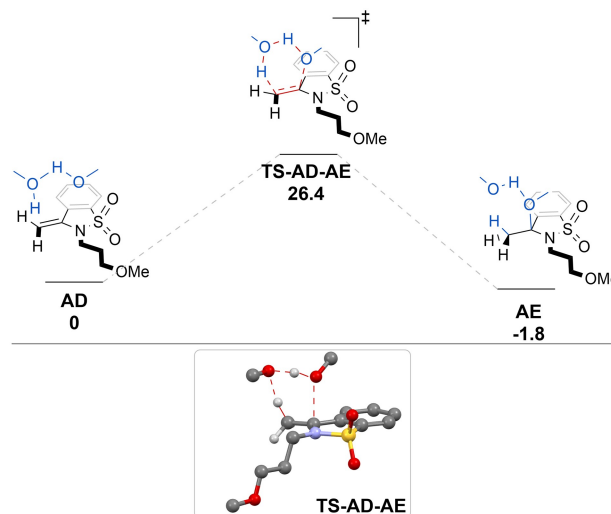
Scheme 9 summarizes experimental and theoretical observation on a catalytic cycle including 1) mono- and di-gold species and 2) the selectivity of the process using terminal and non-terminal alkynes.

Conclusions

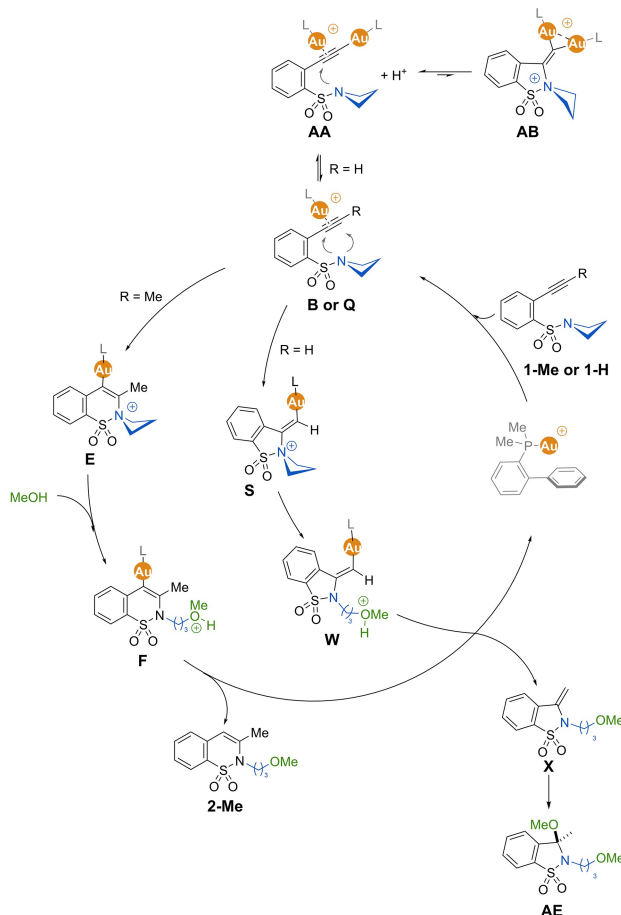
We have computed the full mechanism of benzosultam formation through gold(I)-catalyzed ammoniumiation process in presence of an external nucleophile using (2-alkynyl)phenylsulfonyl azetidines **1-Me** or **1-H** alkynes as model substrates. The study of the reaction using **1-Me** as a non-terminal alkyne, confirms the

⁹Any attempt to locate a transition state led to a high energy cationic intermediate.

¹⁰Calculations modeling a concerted four-membered ring transition state were launched, but no concerted transition state could be located. Only the direct addition of methanol on the carbon center could be found and led to a high barrier.



Scheme 8. Free energy reaction profile (kcal/mol) for the formation of the final aminal **AE** with **1-H** as substrate computed at the B3LYP-D3(DCM)/LANL2TZ(f)/6-311++G**//LANL2DZ/6-31G** level of theory.



Scheme 9. Proposed catalytic cycle for the Au(I) catalyzed benzosultam formation.

ammoniumation based mechanism as the most favored process. Indeed, the nucleophilic addition of the nitrogen to the Au(I)-activated alkyne showed to be clearly favored over the direct ring opening of the azetidine by methanol. As experimentally, the use of terminal alkynes led to the formation of the 5-*exo*-dig sultam instead of the classical 6-*endo*-dig, calculations with the terminal alkyne **1-H** were also studied and, in order to decipher the origin of this reversed regioselectivity, two different scenarios were considered: 1) the classical activation of the alkyne by a single gold(I) complex or, 2) the digold pathway involving the formation of a σ,π -digold acetylide complex. The first scenario revealed that the formation of the 5-membered ring transition state was favored by 2.4 kcal·mol⁻¹ whereas the second scenario was unproductive. In fact, due to the high barrier of the nucleophilic substitution as well as the disfavored formation of the spirocyclic vinyl-ammonium-digold(I) species (*Scheme 7*, **AC** species), the digold pathway is unable to reach the final sultam. However, the formation of such σ,π -digold acetylide is in equilibrium with the monogold species becoming competitive to the productive monogold process. Thus, the digold scenario represents a reversible deactivation pathway accounting for the slow kinetic observed under the experimental conditions. In addition, the small energy difference computed for the formation of the 5- and 6-membered sultams agrees with the loss of selectivity observed when the temperature was increased. Our study also revealed that the rate limiting step of the process is the ring opening of the azetidine by the nucleophile (**E** to **F**) which is consistent with experimental observations, for which steric and electronic properties of the nucleophile drastically influence the kinetic of the reaction.

Overall, the full mechanistic analysis of these complex reactions may facilitate not only the design of new gold(I)-catalyzed ammoniumation process but also the optimization of the selective formation of the amination sultam.

Acknowledgements

We gratefully thank the University of Geneva, the *Swiss National Science Foundation*, the French Ministry of Research, and the CNRS for financial support. We also thank *Carmine Chiancone* for technical support. Open access funding provided by Université de Genève.

Author Contribution Statement

R. P. performed the computational study under the supervision of *A. I. P.-B. R. P.* and *A. A.* co-wrote the draft of the manuscript which was finalized by *R. P., P. P., A. B.* and *A. I. P.-B.* All authors commented on the manuscript.

References

- [1] V. Michelet, F. D. Toste, 'Gold Catalysis: An Homogeneous Approach', *Catalytic Science Series*, Vol. 13, World Scientific, 2014.
- [2] A. S. K. Hashmi, F. D. Toste, 'Modern Gold Catalyzed Synthesis', John Wiley & Sons, 2012.
- [3] A. S. K. Hashmi, 'Gold-Catalyzed Organic Reactions', *Chem. Rev.* **2007**, *107*, 3180–3211.
- [4] A. Fürstner, P. W. Davies, 'Catalytic Carbophilic Activation: Catalysis by Platinum and Gold π Acids', *Angew. Chem. Int. Ed.* **2007**, *46*, 3410–3449.
- [5] D. J. Gorin, F. D. Toste, 'Relativistic effects in homogeneous gold catalysis', *Nature* **2007**, *446*, 395–403.
- [6] Y. Yamamoto, 'From σ - to π -Electrophilic Lewis Acids. Application to Selective Organic Transformations', *J. Org. Chem.* **2007**, *72*, 7817–7831.
- [7] Y. Yamamoto, 'From σ - to π -Electrophilic Lewis Acids. Application to Selective Organic Transformations', *J. Org. Chem.* **2008**, *73*, 5210–5210.
- [8] C. C. Chintawar, A. K. Yadav, A. Kumar, S. P. Sancheti, N. T. Patil, 'Divergent Gold Catalysis: Unlocking Molecular Diversity through Catalyst Control', *Chem. Rev.* **2021**, *121*, 8478–8558.
- [9] Y. Zhang, T. Luo, Z. Yang, 'Strategic innovation in the total synthesis of complex natural products using gold catalysis', *Nat. Prod. Rep.* **2014**, *31*, 489–503.
- [10] R. Dorel, A. M. Echavarren, 'Gold(I)-Catalyzed Activation of Alkynes for the Construction of Molecular Complexity', *Chem. Rev.* **2015**, *115*, 9028–9072.
- [11] H. Duan, S. Sengupta, J. L. Petersen, N. G. Akhmedov, X. Shi, 'Triazole–Au(I) Complexes: A New Class of Catalysts with Improved Thermal Stability and Reactivity for Intermolecular Alkyne Hydroamination', *J. Am. Chem. Soc.* **2009**, *131*, 12100–12102.
- [12] X. Zeng, G. D. Frey, R. Kinjo, B. Donnadiou, G. Bertrand, 'Synthesis of a Simplified Version of Stable Bulky and Rigid Cyclic (Alkyl)(amino)carbenes, and Catalytic Activity of the Ensuing Gold(I) Complex in the Three-Component Preparation of 1,2-Dihydroquinoline Derivatives', *J. Am. Chem. Soc.* **2009**, *131*, 8690–8696.
- [13] X. Zeng, G. D. Frey, S. Kousar, G. Bertrand, 'A Cationic Gold (I) Complex as a General Catalyst for the Intermolecular Hydroamination of Alkynes: Application to the One-Pot Synthesis of Allenes from Two Alkynes and a Sacrificial Amine', *Chem. Eur. J.* **2009**, *15*, 3056–3060.
- [14] K. D. Hesp, M. Stradiotto, 'Stereo- and Regioselective Gold-Catalyzed Hydroamination of Internal Alkynes with Dialkylamines', *J. Am. Chem. Soc.* **2010**, *132*, 18026–18029.

- [15] L. Biasiolo, L. Belpassi, C. A. Gaggioli, A. Macchioni, F. Tarantelli, G. Ciancaleoni, D. Zuccaccia, 'Cyclization of 2-Alkynyldimethylaniline on Gold(I) Cationic and Neutral Complexes', *Organometallics* **2016**, *35*, 595–604.
- [16] X. Zeng, R. Kinjo, B. Donnadiu, G. Bertrand, 'Serendipitous Discovery of the Catalytic Hydroammoniumation and Methylation of Alkynes', *Angew. Chem. Int. Ed.* **2010**, *49*, 942–945.
- [17] I. Nakamura, U. Yamagishi, D. Song, S. Konta, Y. Yamamoto, 'Gold- and Indium-Catalyzed Synthesis of 3- and 6-Sulfonylindoles from *ortho*-Alkynyl-*N*-sulfonylanilines', *Angew. Chem. Int. Ed.* **2007**, *46*, 2284–2287.
- [18] I. Nakamura, U. Yamagishi, D. Song, S. Konta, Y. Yamamoto, 'Synthesis of 3- and 6-Sulfonylindoles from *ortho*-Alkynyl-*N*-sulfonylanilines by the Use of Lewis Acidic Transition-Metal Catalysts', *Chem. Asian J.* **2008**, *3*, 285–295.
- [19] Y. J. Hong, D. J. Tantillo, 'Does Gold as a Substituent Accelerate [3,3] Sigmatropic Shifts?', *Organometallics* **2011**, *30*, 5825–5831.
- [20] H.-S. Yeom, E. So, S. Shin, 'Gold-Catalyzed Synthesis of 3-Pyrrolidinones and Nitrones from *N*-Sulfonyl Hydroxylamines via Oxygen-Transfer Redox and 1,3-Sulfonyl Migration', *Chem. Eur. J.* **2011**, *17*, 1764–1767.
- [21] W. T. Teo, W. Rao, M. J. Koh, P. W. H. Chan, 'Gold-Catalyzed Domino Aminocyclization/1,3-Sulfonyl Migration of *N*-Substituted *N*-Sulfonyl-aminobut-3-yn-2-ols to 1-Substituted 3-Sulfonyl-1*H*-pyrroles', *J. Org. Chem.* **2013**, *78*, 7508–7517.
- [22] J. Liu, P. Chakraborty, H. Zhang, L. Zhong, Z.-X. Wang, X. Huang, 'Gold-Catalyzed Atom-Economic Synthesis of Sulfone-Containing Pyrrolo[2,1-*a*]isoquinolines from DYNAMIDES: Evidence for Consecutive Sulfonyl Migration', *ACS Catal.* **2019**, *9*, 2610–2617.
- [23] F. Wu, L. Chen, Y. Wang, S. Zhu, 'Gold-catalyzed generation of azafulvenium from an enyne sulfonamide: rapid access to fully substituted pyrroles', *Org. Chem. Front.* **2019**, *6*, 480–485.
- [24] T. Sakai, C. Okumura, M. Futamura, N. Noda, A. Nagae, C. Kitamoto, M. Kamiya, Y. Mori, 'Gold(I)-Catalyzed Cyclization-3-Aza-Cope-Mannich Cascade and Its Application to the Synthesis of Cephalotaxine', *Org. Lett.* **2021**, *23*, 4391–4395.
- [25] S. Miaskiewicz, B. Gaillard, N. Kern, J.-M. Weibel, P. Pale, A. Blanc, 'Gold(I)-Catalyzed *N*-Desulfonylative Amination versus *N*-to-*O* 1,5-Sulfonyl Migration: A Versatile Approach to 1-Azabicycloalkanes', *Angew. Chem. Int. Ed.* **2016**, *55*, 9088–9092.
- [26] S. Miaskiewicz, J.-M. Weibel, P. Pale, A. Blanc, 'Gold(I)-Catalyzed Cyclization/Nucleophilic Substitution of 1-(*N*-Sulfonylazetid-2-yl) Ynones into *N*-Sulfonylpyrrolin-4-ones', *Org. Lett.* **2016**, *18*, 844–847.
- [27] R. Pertschi, S. Miaskiewicz, J.-M. Weibel, P. Pale, A. Blanc, 'Gold(I)-Catalyzed Cascade: Synthesis of 2,5-Disubstituted Pyrroles from *N*-Sulfonyl-2-(1-ethoxypropargyl)azetidines through Cyclization/Nucleophilic Substitution/Elimination', *Synthesis* **2017**, *49*, 4151–4162.
- [28] F. Sirindil, S. Golling, R. Lamare, J.-M. Weibel, P. Pale, A. Blanc, 'Synthesis of Indolizine and Pyrrolo[1,2-*a*]azepine Derivatives via a Gold(I)-Catalyzed Three-Step Cascade', *Org. Lett.* **2019**, *21*, 8997–9000.
- [29] F. Sirindil, J.-M. Weibel, P. Pale, A. Blanc, 'Total Synthesis of Rhazinilam through Gold-Catalyzed Cycloisomerization-Sulfonyl Migration and Palladium-Catalyzed Suzuki-Miyaura Coupling of Pyrrolyl Sulfonates', *Org. Lett.* **2019**, *21*, 5542–5546.
- [30] R. Pertschi, S. Miaskiewicz, N. Kern, J.-M. Weibel, P. Pale, A. Blanc, 'Gold(I)-catalyzed divergent and diastereoselective synthesis of azepines by ammoniumation/ring-expansion reactions', *Chem. Catal.* **2021**, *1*, 129–145.
- [31] R. Pertschi, J.-M. Weibel, P. Pale, A. Blanc, 'Benzosultam Synthesis by Gold(I)-Catalyzed Ammonium Formation/Nucleophilic Substitution', *Org. Lett.* **2019**, *21*, 5616–5620.
- [32] Gaussian 09, Revision A.02, M. J. Frisch, G. W. Trucks, H. B. Schlegel, G. E. Scuseria, M. A. Robb, J. R. Cheeseman, G. Scalmani, V. Barone, G. A. Petersson, H. Nakatsuji, X. Li, M. Caricato, A. Marenich, J. Bloino, B. G. Janesko, R. Gomperts, B. Mennucci, H. P. Hratchian, J. V. Ortiz, A. F. Izmaylov, J. L. Sonnenberg, D. Williams-Young, F. Ding, F. Lipparini, F. Egidi, J. Goings, B. Peng, A. Petrone, T. Henderson, D. Ranasinghe, V. G. Zakrzewski, J. Gao, N. Rega, G. Zheng, W. Liang, M. Hada, M. Ehara, K. Toyota, R. Fukuda, J. Hasegawa, M. Ishida, T. Nakajima, Y. Honda, O. Kitao, H. Nakai, T. Vreven, K. Throssell, J. A. Montgomery Jr., J. E. Peralta, F. Ogliaro, M. Bearpark, J. J. Heyd, E. Brothers, K. N. Kudin, V. N. Staroverov, T. Keith, R. Kobayashi, J. Normand, K. Raghavachari, A. Rendell, J. C. Burant, S. S. Iyengar, J. Tomasi, M. Cossi, J. M. Millam, M. Klene, C. Adamo, R. Cammi, J. W. Ochterski, R. L. Martin, K. Morokuma, O. Farkas, J. B. Foresman, D. J. Fox, Gaussian, Inc., Wallingford CT, 2016.
- [33] A. D. Becke, 'Density-functional thermochemistry. III. The role of exact exchange', *J. Chem. Phys.* **1993**, *98*, 5648.
- [34] S. Grimme, J. Antony, S. Ehrlich, H. Krieg, 'A consistent and accurate *ab initio* parametrization of density functional dispersion correction (DFT-D) for the 94 elements H–Pu', *J. Chem. Phys.* **2010**, *132*, 154104.
- [35] C. Lee, W. Yang, R. G. Parr, 'Development of the Colle-Salvetti correlation-energy formula into a functional of the electron density', *Phys. Rev. B* **1988**, *37*, 785.
- [36] P. J. Stephens, F. J. Devlin, C. F. Chabalowski, M. J. Frisch, 'Ab initio Calculation of Vibrational Absorption and Circular Dichroism Spectra Using Density Functional Force Fields', *J. Phys. Chem.* **1994**, *98*, 11623–11627.
- [37] P. J. Hay, W. R. Wadt, 'Ab initio effective core potentials for molecular calculations. Potentials for the transition metal atoms Sc to Hg', *J. Chem. Phys.* **1985**, *82*, 270–283.
- [38] P. C. Hariharan, J. A. Pople, 'The influence of polarization functions on molecular orbital hydrogenation energies', *Theor. Chim. Acta* **1973**, *28*, 213–222.
- [39] W. J. Hehre, R. Ditchfield, J. A. Pople, 'Self-Consistent Molecular Orbital Methods. XII. Further Extensions of Gaussian-Type Basis Sets for Use in Molecular Orbital Studies of Organic Molecules', *J. Chem. Phys.* **1972**, *56*, 2257–2261.
- [40] M. M. Francl, W. J. Pietro, W. J. Hehre, J. S. Binkley, M. S. Gordon, D. J. DeFrees, J. A. Pople, 'Self-consistent molecular orbital methods. XXII. A polarization-type basis set for second-row elements', *J. Chem. Phys.* **1982**, *77*, 3654–3665.
- [41] T. Clark, J. Chandrasekhar, G. W. Spitznagel, P. von Ragué Schleyer, 'Efficient diffuse function-augmented basis sets for anion calculations. III. The 3–21+G basis set for first-row elements, Li–F', *J. Comput. Chem.* **1983**, *4*, 294–301.

- [42] R. Ditchfield, W. J. Hehre, J. A. Pople, 'Self-Consistent Molecular-Orbital Methods. IX. An Extended Gaussian-Type Basis for Molecular Orbital Studies for Organic Molecules', *J. Chem. Phys.* **1971**, *54*, 724–728.
- [43] G. W. Spitznagel, T. Clark, P. von Ragué Schleyer, W. J. Hehre, 'An evaluation of the performance of diffuse function-augmented basis sets for second row elements, Na–Cl', *J. Comput. Chem.* **1987**, *8*, 1109–1116.
- [44] M. S. Gordon, J. S. Binkley, J. A. Pople, W. J. Pietro, W. J. Hehre, 'Self-consistent molecular-orbital methods. 22. Small split-valence basis sets for second-row elements', *J. Am. Chem. Soc.* **1982**, *104*, 2797–2803.
- [45] L. E. Roy, P. J. Hay, R. L. Martin, 'Revised Basis Sets for the LANL Effective Core Potentials', *J. Chem. Theory Comput.* **2008**, *4*, 1029–1031.
- [46] R. Krishnan, J. S. Binkley, R. Seeger, J. A. Pople, 'Self-consistent molecular orbital methods. XX. A basis set for correlated wave functions', *J. Chem. Phys.* **1980**, *72*, 650–654.
- [47] K. Fukui, 'The path of chemical reactions - the IRC approach', *Acc. Chem. Res.* **1981**, *14*, 363–368.
- [48] H. Hratchian, H. Schlegel, 'Finding minima, transition states, and following reaction pathways on ab initio potential energy surfaces', Chapt. 10 in 'Theory and Applications of Computational Chemistry: The First 40 Years', Eds. C. E. Dykstra, G. Frenking, K. S. Kim, G. E. Scuseria, Elsevier B. V., 2005, pp. 195–249.
- [49] R. Pertschi, P. Wagner, N. Ghosh, V. Gandon, G. Blond, 'Gold(I)-Catalyzed Synthesis of Furofurans: Insight into Hetero-Diels–Alder Reactions', *Org. Lett.* **2019**, *21*, 6084–6088.
- [50] P. Wagner, N. Ghosh, V. Gandon, G. Blond, 'Solvent Effect in Gold(I)-Catalyzed Domino Reaction: Access to Furofurans', *Org. Lett.* **2020**, *22*, 7333–7337.
- [51] G. Zhao, C. Roudaut, V. Gandon, M. Alami, O. Provot, 'Synthesis of 2-substituted indoles through cyclization and demethylation of 2-alkynyldimethylanilines by ethanol', *Green Chem.* **2019**, *21*, 4204–4210.
- [52] A. S. K. Hashmi, A. M. Schuster, F. Rominger, 'Gold Catalysis: Isolation of Vinylgold Complexes Derived from Alkynes', *Angew. Chem. Int. Ed.* **2009**, *48*, 8247–8249.
- [53] T. J. Brown, R. A. Widenhoefer, 'Cationic Gold(I) π -Complexes of Terminal Alkynes and Their Conversion to Dinuclear σ,π -Acetylide Complexes', *Organometallics* **2011**, *30*, 6003–6009.
- [54] A. Gómez-Suárez, S. P. Nolan, 'Dinuclear Gold Catalysis: Are Two Gold Centers Better than One?', *Angew. Chem. Int. Ed.* **2012**, *51*, 8156–8159.
- [55] L. Jašíková, J. Roithová, 'Interaction of Gold Acetylides with Gold(I) or Silver(I) Cations', *Organometallics* **2013**, *32*, 7025–7033.
- [56] M. Veguillas, G. M. Rosair, M. W. P. Bebbington, A.-L. Lee, 'Silver Effect in Regiodivergent Gold-Catalyzed Hydroaminations', *ACS Catal.* **2019**, *9*, 2552–2557.
- [57] T. A. C. A. Bayrakdar, T. Scattolin, X. Ma, S. P. Nolan, 'Dinuclear gold(I) complexes: from bonding to applications', *Chem. Soc. Rev.* **2020**, *49*, 7044–7100.
- [58] J. Wang, S. Lv, H. Chen, M. Shi, J. Zhang, 'Isolation and characterization of *gem*-diaurated species having two C–Au σ bonds in gold(I)-activated amidinium of alkynes', *Dalton Trans.* **2016**, *45*, 17091–17094.
- [59] J. Wang, K. Yuan, G. Wang, Y. Liu, J. Zhang, 'Catalytic Arylative *Endo* Cyclization of Gold Acetylides: Access to 3,4-Diphenyl Isoquinoline, 2,3-Diphenyl Indole, and Mesoionic Normal NHC–Gold Complex', *Chem. Eur. J.* **2021**, *27*, 212–217.
- [60] D. V. Partyka, T. J. Robilotto, M. Zeller, A. D. Hunter, T. G. Gray, 'Dialkylbiarylphosphine Complexes of Gold(I) Halides. Gold–Aryl π -Interactions in the Solid State', *Organometallics* **2008**, *27*, 28–32.
- [61] S. Ferrer, A. M. Echavarren, 'Role of σ,π -Digold(I) Alkyne Complexes in Reactions of Enynes', *Organometallics* **2018**, *37*, 781–786.
- [62] A. Simonneau, F. Jaroschik, D. Lesage, M. Karanik, R. Guillot, M. Malacria, J.-C. Tabet, J.-P. Goddard, L. Fensterbank, V. Gandon, Y. Gimbert, 'Tracking gold acetylides in gold(I)-catalyzed cycloisomerization reactions of enynes', *Chem. Sci.* **2011**, *2*, 2417–2422.

Received July 15, 2021

Accepted September 2, 2021